Identification of the Catalytic Residues of AroA (*Enol*pyruvylshikimate 3-Phosphate Synthase) Using Partitioning Analysis†

Shehadeh Mizyed,‡,§ Jennifer E. I. Wright,‡,§ Bartosz Byczynski,‡,§ and Paul J. Berti*,‡,§,||

Department of Chemistry, Department of Biochemistry, and the Antimicrobial Research Centre, McMaster University, 1280 Main Street West, Hamilton, Ontario, L8S 4M1, Canada

Received November 21, 2002; Revised Manuscript Received May 1, 2003

ABSTRACT: AroA (EPSP synthase) catalyzes carboxyvinyl transfer through addition of shikimate 3-phosphate (S3P) to phospho*enol*pyruvate (PEP) to form a tetrahedral intermediate (THI), followed by phosphate elimination to give *enol*pyruvylshikimate 3-phosphate (EPSP). A novel approach, partitioning analysis, was used to elucidate the roles of catalytic residues in each step of the reaction. Partitioning analysis involved trapping and purifying [1-^{14}C]THI, degrading it with AroA, and quantitating the products. Wild-type AroA gave a partitioning factor, f(PEP) = 0.25 ± 0.02 at pH 7.5, where f(PEP) = [[1-^{14}C]PEP]/([[1-^{14}C]PEP] + [[1-^{14}C]EPSP]). Eighteen mutations were made to 14 amino acids to discover which residues preferentially catalyzed either the addition or the elimination step. Mutating a residue catalyzing one step (e.g., addition) should change f(PEP) to favor the opposite step (e.g., elimination). No mutants caused large changes in f(PEP), with experimental values from 0.07 to 0.41. This implied that there are no side chains that catalyze only addition or elimination, which further implied that the same residues are general acid/base catalysts in both forward and reverse THI breakdown. Only Lys22 (protonating S3P hydroxyl or phosphate) and Glu341 (deprotonating C3 of PEP) are correctly situated in the active site. In the overall reaction, Lys22 would act as a general base during addition, while Glu341 would act as a general acid. Almost half of the mutations (eight of 18) caused a >1000-fold decrease in specific activity, demonstrating that a large number of residues are important for transition state stabilization, "ensemble catalysis", in contrast to some enzymes where a single amino acid can be responsible for up to 10^8-fold catalytic enhancement.

The enzymes AroA[1] and MurA have been studied extensively because of their novel catalytic mechanisms and their potential as targets for antimicrobial agents. They are the only two enzymes known to catalyze carboxyvinyl transfer reactions (Figure 1). AroA is part of the shikimate pathway that produces the aromatic amino acids and most other aromatic compounds in bacteria, plants, and apicomplexa (*1*); MurA is part of the peptidoglycan biosynthesis pathway in bacteria. Both are targets of commercially important inhibitors. EPSP synthase, the plant ortholog of AroA, is the target of glyphosate (*N*-(phosphonomethyl)glycine), the active ingredient in the herbicide Roundup (*1*), while MurA is inhibited by the antibiotic fosfomycin (*2*).

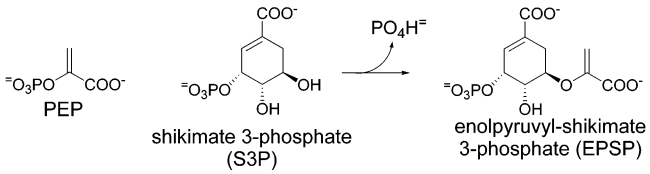

FIGURE 1: Reaction catalyzed by AroA.

Both enzymes have been the subject of numerous mechanistic investigations. In a seminal series of papers, Anderson and Johnson (*3*−*7*) demonstrated that carboxyvinyl transfer proceeds through an addition/elimination pathway that passes through a noncovalent tetrahedral intermediate (THI). MurA was later shown to follow the same reaction pathway (*8*−*12*). Kinetic analyses of mutants of AroA and MurA have allowed some side chains to be identified as essential or nonessential, but it is not possible to tell from studies of the overall reaction which of the two steps, addition or elimination, is affected by the mutation and therefore what role the mutated residue might play. Both addition and elimination are subject to both general acid and general base catalysis.

We set out to identify the catalytically important residues in *Escherichia coli* AroA through partitioning analysis. Putative catalytic residues were identified in enzyme·substrate and enzyme·inhibitor cocrystal structures (*11*, *13*−*19*) and mutated. The AroA THI was trapped, purified, and reacted with either wild-type AroA or one of 18 mutants, and the product distribution was examined to determine the

† This work was supported by the Canadian Institutes of Health Research, as well as graduate scholarships from the Natural Sciences and Engineering Research Council of Canada (J.E.I.W. and B.B.).

* To whom correspondence should be addressed. Telephone: (905) 525-9140 ext. 23479. Fax: (905) 522-2509. E-mail: berti@mcmaster.ca.

‡ Department of Chemistry.

§ Antimicrobial Research Centre.

|| Department of Biochemistry.

[1] Abbreviations: AroA, EPSP synthase; $AroA_{H6}$, AroA with a C-terminal extension terminating with His_6; EPSP, *enol*pyruvylshikimate 3-phosphate; EP-UDP-GlcNAc, *enol*pyruvyluridine diphosphate *N*-acetyl-glucosamine; MurA, EP-UDP-GlcNAc synthase; F-THI, 3-fluoro-derivative of the MurA THI; IPTG, isopropyl-β-D-thiogalactopyranoside; PEP, phospho*enol*pyruvate; Pi, inorganic phosphate; S3P, shikimate 3-phosphate; THI, tetrahedral intermediate; TS, transition state; UDP-GlcNAc, uridine diphosphate *N*-acetylglucosamine; $\Delta\Delta G^{\ddagger}$, change in the free energy of activation relative to $AroA_{H6}$.

10.1021/bi027217l CCC: $25.00
Published on Web 05/23/2003

effects on the forward and reverse reactions. THI partitions back to S3P + PEP or forward to EPSP + phosphate in a ratio of 1:3 with wild-type AroA. In mutants, changes in transition state (TS) stabilization of the addition or elimination steps would be reflected by changes in partitioning. These changes would show which step of the reaction was promoted by a given amino acid residue. To the best of our knowledge, this partitioning analysis approach with a reintroduced catalytic intermediate has not been used before. Complete free energy profiles of several enzymes have been elucidated (e.g., see refs *5*, *20*, and *21*). These profiles describe all internal equilibria and partitioning factors for each step of the reaction but require large, sometimes heroic efforts to determine. The ability to synthesize and purify AroA THI, albeit only ca. 50 nmol per synthesis, allowed us to examine the roles of amino acids more directly by partitioning analysis.

Perhaps surprisingly, no mutation caused large changes in partitioning despite often large decreases in specific activity. This is evidence that the general acid and general base catalysts in THI breakdown are the same residues for the forward and reverse reactions.

EXPERIMENTAL PROCEDURES

Wild-Type AroA. Recombinant *E. coli* AroA was PCR amplified from *E. coli* strain DH5α and ligated into pET24d (Novagen, Inc.), replacing the *NcoI*−*BamHI* fragment. The insert was sequenced and found to be identical to a Genbank entry, accession AE000193 in the region of 2141−3424. The AroA-containing plasmid was transformed into *E. coli* strain BL21*(DE3) (Invitrogen). Wild-type AroA was expressed and purified as described previously (*22*), except cells were lysed in a French Press after addition of 100 μg/mL DNAase and RNAase and 2 μg/mL phenylmethylsulfonyl fluoride. The final purification step used Q-Sepharose (Amersham Biosciences) rather than Mono-Q. All steps were performed at 0−4 °C. The identity of AroA was confirmed by DNA sequencing and mass spectrometry ($M_{r(calc)}$ = 46 096, $M_{r(obs)}$ = 46 104).

His-Tagged AroA (AroA$_{H6}$). $AroA_{H6}$ contained a 22 amino acid C-terminal extension terminating with His_6, created by a frame-shift mutation that removed the stop codon and brought the C-terminal extension of the pET24d vector into register. Mutagenesis was done using a Quikchange-like strategy (Stratagene) (see Supporting Information). $AroA_{H6}$ was expressed as AroA, but the lysis buffer did not contain EDTA. It was affinity purified using a 30 mL Chelating-Sepharose (Amersham Biosciences) column charged with $NiSO_4$. Pelleted cells were resuspended in ice-cold lysis buffer, and all subsequent steps were performed at 0−4 °C. After lysis and centrifugation, 20 mL of cell lysate was applied to the column at a flow rate of 1 mL/min, followed by a wash with ca. 50 mL of wash buffer (50 mM Tris·HCl, pH 7.5, 20 mM imidazole, 300 mM NaCl) until A_{254} returned to zero. $AroA_{H6}$ was eluted by stepping to the elution buffer (as wash buffer, but 500 mM imidazole). The buffer was exchanged by ultrafiltration to 50 mM HEPES, 50 mM KCl, pH 7.0, and the protein was concentrated to ca. 1 mM (48 mg/mL). Commercial protease inhibitor cocktail was added, and $AroA_{H6}$ was stored on ice. The concentrated protein precipitated if frozen. The protein was >98% pure as judged by SDS/PAGE. The identity of $AroA_{H6}$ was confirmed by DNA sequencing and mass spectrometry ($M_{r(calc)}$ = 48 546, $M_{r(obs)}$ = 48 562). Protein concentration was determined using $\epsilon_{280} = 3.55 \times 10^4\ M^{-1}\ cm^{-1}$, which was determined by the method of Edelhoch (*23*, *24*). The concentration of active $AroA_{H6}$ was determined by fluorescence titration using S3P and glyphosate (*25*) and used to calculate k_{cat}/K_M for THI breakdown.

Mutant AroA$_{H6}$s. Single site mutants of $AroA_{H6}$ were created using the same mutagenesis strategy as above (see Supporting Information). Protein expression was as with $AroA_{H6}$, except that protein expression was induced at 18 °C for 40 h instead of 37 °C. Purification was as for $AroA_{H6}$, but using pre-packed 1 mL HiTrap Chelating-Sepharose (Amersham Biosciences) columns. Centrifuged cell lysate (5−25 mL) was applied to the column, which was washed with 25 column volumes of wash buffer to remove all wild-type AroA before elution. The identity of each mutant was confirmed by DNA sequencing and mass spectrometry (see Supporting Information). The wild-type value of ϵ_{280} was used as there were no mutants of aromatic or Cys residues. The proteins were >99% pure as determined by SDS/PAGE. Because of decreased glyphosate affinity in many mutants, active site concentrations could not be obtained. All specific activities are therefore reported in units of (μmol min^{-1}) mg^{-1}.

Shikimate 3-Phosphate. Shikimate 3-phosphate was synthesized as described previously (*26*), except purification was performed using DEAE-Sephadex and elution with 30 mM to 1 M ammonium formate, pH 8.0.

[1-^{14}C]PEP. A 100 μL solution containing [1-^{14}C]pyruvate (3.7 mM, 10 μCi) was incubated overnight with 3.7 mM ATP, 50 mM potassium phosphate, 10 mM $MgCl_2$, 5 mM KCl, pH 7.5, 10 U inorganic pyrophosphatase, and 0.3 U pyruvate phosphate dikinase (a gift from D. Dunaway-Mariano, University of New Mexico). PEP was purified using a 1 mL Q-Sepharose HP (Amersham Biosciences) anion exchange column, with a gradient from 100 to 500 mM NH_4·HCO_3, pH 10.

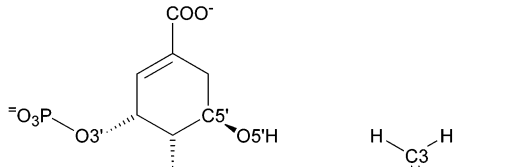

[^{33}P]PEP. [^{33}P]PEP was synthesized as described previously (*27*). It was purified by C18 reverse phase chromatography, with PEP and pyruvate coeluting in 50 mM triethylammonium acetate, pH 6.0, 1 mL/min, then stepping to 20% MeOH to elute ATP. It was further purified with Hitrap-Q (Amersham Biosciences) anion exchange chromatography, in 100−500 mM NH_4·HCO_3, pH 10.

Rate Assays. ^{33}P-Based Assay. Reaction rates were measured by separation of [^{33}P]PEP from [^{33}P]phosphate by anion exchange thin-layer chromatography on polyethyleneimine cellulose, with 2 M sodium acetate, pH 5.0 as solvent (*28*) and detection of radioactivity by storage phosphor autora-

diography. Specific activities were determined with 3 mM S3P and 8 mM PEP in 50 mM Tris·HCl, pH 7.5, 100 mM KCl, at 25 °C, with 400−600 cpm of ^{33}P per time point, enzyme concentrations of 40 nM to 40 μM, and reaction times of 20 min to 6 h. These substrate concentrations are near-saturating for wild-type enzyme; K_Ms were not determined for mutants. Rates were also determined by following the appearance of phosphate using the spectrophotometric Malachite Green assay (*29*).

THI Synthesis. AroA THI was synthesized by quenching an equilibrated reaction mixture with base, similarly to previous experiments (*5*, *7*), but with harsher conditions to denature $AroA_{H6}$. A 100 μL reaction mixture contained 1 mM enzyme, 1 mM S3P, 0.5 mM PEP, 50 mM potassium phosphate, pH 7.5, and 0.1−0.2 μCi of [1-^{14}C]PEP. Enzyme was added last, incubated for 2 min at room temperature, and then quenched by quickly adding the reaction mixture to 20 μL of 2 N KOH/50 μL (KOH-saturated 2-propanol). This was extracted with 250 μL of $CHCl_3$, vortexed vigorously for 30 s, and centrifuged at 16 000*g* for 1 min, and the (small) aqueous layer was pipetted from the top. The $CHCl_3$ layer and large overlaying layer of precipitated protein were extracted with 200 μL of 0.4 N KOH/100 μL (KOH-saturated 2-propanol). After vortexing and centrifuging, this was combined with the first aqueous fraction. The combined aqueous fractions were extracted 2−5 times with 250 μL of $CHCl_3$, until no more protein precipitate formed at the aqueous/organic interface. The aqueous layer was then diluted to 2 mL with water and purified on a Mono-Q anion exchange column (5 × 50 mm, Amersham Biosciences) with a gradient of 50 mM to 1 M Et_3N·HCl, pH 9.0, over 20 min, at 0.5 mL/min, with A_{240} detection. Approximate elution times were pyruvate, 11 min; S3P, 18 min; PEP, 21.5 min; EPSP, 23 min; and THI, 28 min. Purified THI was stored at 0 °C.

Partitioning Experiments. For most partitioning experiments, purified THI containing ca. 1500 cpm of ^{14}C (typically 125 μL) was added to enzyme and buffer to a final volume of 1900 μL of 50 mM Tris·HCl, 50 mM KCl, 50 mM Et_3N·HCl, pH 7.5, at 25 °C. Because of the high pH of the THI buffer (pH 9.0), Tris·HCl buffer at pH 7.0 was used to achieve pH 7.5. Enzyme concentrations of 175 pM ($AroA_{H6}$) to 15 nM were used to degrade THI. KOH was added to 0.1 N to stop the reaction. HPLC was as for THI synthesis, and 1 mL fractions were collected, centered on the retention time of each peak, then 10 mL of scintillation fluid was added (Liquiscint, National Diagnostics), and ^{14}C was counted 2 × 5 min. Blanks consisting of elution buffer with the same composition were subtracted. The high salt concentration in the elution buffer caused a <1% decrease in counting efficiency. The radioactivity in pyruvate (diagnostic of nonenzymatic THI breakdown), PEP, EPSP, and THI were determined. The fraction of PEP formed from THI was calculated: f(PEP) = [[1-^{14}C]PEP]/([[1-^{14}C]PEP] + [[1-^{14}C]-EPSP]).

The pH-dependence of partitioning with $AroA_{H6}$ was also examined using the same procedure as above. The added buffer generally had a higher or lower pH than the desired final pH to compensate for the buffering capacity of Et_3N·HCl from the THI buffer. The pH was determined using test mixtures containing the same buffer composition as the reaction mixtures. The following buffers were used, at 50 mM concentration: pH < 6.2, sodium citrate; pH 6.4−9.4, Bis-Trispropane; pH 9.5−11.0, glycine; pH >11.0, KOH; also Tris·HCl at pH 7.5.

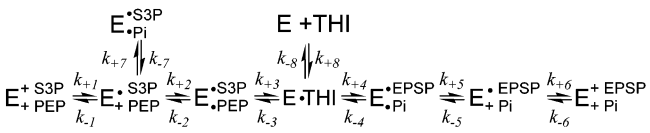

FIGURE 2: Kinetic mechanism of AroA. The mechanism and microscopic rate constants used are from ref *5*, except for k_{+8} and k_{-8} (see text). E = AroA and other abbreviations are as defined in the text.

Nonenzymatic THI breakdown, which would form [1-^{14}C]-pyruvate, was negligible during all partitioning experiments. At low pH, as the rate of nonenzymatic breakdown increased, [$AroA_{H6}$] was raised to ensure the enzymatic reaction was dominant.

AroA·THI Model. A model of the AroA·THI complex was created based on the X-ray crystal structures of AroA·S3P·glyphosate (PDB 1G6S) and MurA·F-THI (PDB 1A2N). F-THI contains a fluoro substituent on the methyl group (C3). Superposition of C_αs of the AroA and MurA structures gave an rms deviation of 3.2 Å and nearly superimposed ligand atoms, with 0.8 Å between the reactive hydroxyls for S3P (O5′H) and UDP-GlcNAc (O3′′H). The THI was generated by bonding S3P O5′H to the C2 atom of the fluoro-THI, deleting the fluorine atom, then performing a molecular mechanical optimization using the Merck mmff94 (*30*) force field, as implemented in MOE (Chemical Computing Group Inc.). Two water molecules in the active site were retained in the model. As this model was only meant as a guide for identifying potential catalytic residues, no further optimizations were performed. An all-atom superposition of the protein structures of the original AroA structure (1G6S) with the optimized AroA·THI structure gave an rms deviation of 0.6 Å.

Numerical Simulation of Partitioning. Because all enzyme-bound intermediates are partially equilibrated in the published kinetic mechanism (*5*), it was necessary to perform numerical simulations to provide a basis for interpreting f(PEP). The program KinTekSim (KinTek Corp.), an implementation of Kinsim (*31*), was used. The previously reported mechanism and microscopic rate constants (*5*) were used, with uncomplexed THI added (Figure 2). The values of k_{+8} and k_{-8} are unknown, except that $k_{+8} \geq 5 \times 10^7$ M^{-1} s^{-1}, the reported value of k_{cat}/K_M. They have no effect on partitioning because they do not discriminate between the forward and the reverse reactions. Simulations used $k_{+8} = 6.5 \times 10^8$ M^{-1} s^{-1} (= k_{+1}, the rate of S3P association), $k_{-8} = 13$ s^{-1} (to give k_{cat}/K_M equal to the previously reported value), with 400 pM AroA and 2 μM THI. Transition state or intermediate energies were changed by adjusting the relevant microscopic rate constants. For example, to increase the TS energy for the elimination reaction by 1.3 kcal/mol, k_{+4} and k_{-4} were decreased 10-fold. The equilibrium ordered kinetic mechanism in the numerical simulations is somewhat incorrect in that more recent kinetic investigations support a random kinetic mechanism with highly synergistic substrate binding (refs *32* and *33* and unpublished results). However, under the low [THI] conditions used here, the first dissociation of a substrate or product molecule is essentially irreversible,

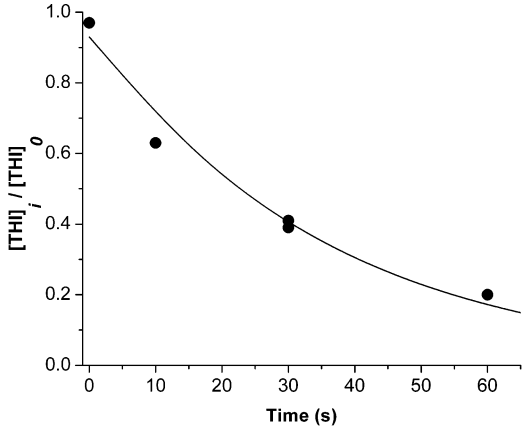

FIGURE 3: Enzymatic THI breakdown by $AroA_{H6}$. $[THI]_i/[THI]_0$ = fraction of THI remaining at time = *i*. [1-^{14}C]THI was 97% pure at $t = 0$. [$AroA_{H6}$] = 200 pM, [THI] ≈ 2 μM, 50 mM Tris·HCl, 50 mM KCl, and 50 mM Et_3N·HCl, pH 7.5.

and the exact random versus ordered mechanism will not affect the partitioning results.

RESULTS

Enzymes. Wild type *E. coli* AroA, $AroA_{H6}$ (containing a C-terminal His_6), and 18 mutants of $AroA_{H6}$ were cloned, expressed, and purified, and their identities were confirmed by DNA sequencing and mass spectrometry. Yields of most purified mutants were within 10% of $AroA_{H6}$ (ca. 30 mg/L of culture), except for D49A (200-fold reduction), R100M (400-fold), Y200F (350-fold), and R386M (1300-fold). Low protein yields likely indicated lower stability because (i) expression and purification conditions were the same for all mutants, (ii) purification did not depend on correct folding, and (iii) the only sequence differences between mutants and $AroA_{H6}$ were one codon substitutions.

Affinity purification with the His_6 tag ensured that constitutively expressed wild-type AroA was effectively removed, as demonstrated by the fact that several mutants had very low specific activity. For the two mutants with very low specific activity (D313N, 16 000-fold reduction, D49A, 21 000-fold), the activity assay involved monitoring the conversion of [^{33}P]PEP to [^{33}P]phosphate for up to 6 h at up to 40 μM enzyme. PEP is stable under these conditions, but microscopic amounts of contaminating enzymes (e.g., wild-type AroA or phosphatases) could account for the observed rate. Thus, for these two highly inactive enzymes, the reported specific activities represent an upper limit of the true values.

THI Synthesis and Breakdown. THI was synthesized in yields of 5−10% relative to [PEP] (i.e., 2.5−5% relative to [$AroA_{H6}$]). Isolated THI was shown to be 97% pure by HPLC, using UV absorbance and in-line radioactivity detection (data not shown). AroA-catalyzed THI breakdown fit well to a first-order decay, with a fitted value of k_{cat}/K_M = 1.4 (±0.1) × 10^8 M^{-1} s^{-1} (Figure 3). This provides an estimate of the lower limit of k_{cat}/K_M[2] and is in good agreement with the previously reported value of 5 × 10^7 M^{-1} s^{-1} (*6*). This is faster than PEP binding (1.5 × 10^7 M^{-1} s^{-1}) and only slightly slower than EPSP (2 × 10^8 M^{-1} s^{-1}) or S3P (6.5 × 10^8 M^{-1} s^{-1}) binding (*5*), indicating that the THI is a kinetically competent intermediate (*3*). The proportion of PEP formed in the reaction, *f*(PEP), at pH 7.5 was 0.25 ± 0.02. It was similar with wild-type AroA, *f*(PEP) = 0.24 ± 0.001. At pH 7.0, *f*(PEP) = 0.17 (see below) in excellent agreement with *f*(PEP) ≈ 0.19 (Figure 2 from ref *6*), as well as *f*(PEP) calculated from the reported microscopic rate constants, *f*(PEP) = 0.17 (*5*).

Experimental Rates. Wild-type AroA gave kinetic constants similar to those reported previously (data not shown), and $AroA_{H6}$ was almost identical to wild-type AroA (Table 1 and unpublished data). We found activity in all mutants (Table 1). Mutants at some of the same positions as reported here have been described previously (*34*−*41*), and several were described as completely inactive. There were three main differences from previous studies that may have increased our ability to detect activity. (i) All mutant proteins were expressed at 18 °C rather than 37 °C. This was done after initial attempts to express K22A at 37 °C yielded no

Table 1: Partitioning Factors and Specific Activity for Wild Type and Mutant AroAs

enzyme[a]	*f*(PEP)[b]	specific activity ((μmol min^{-1}) mg^{-1})[c]	% conservation in AroAs[d]	MurA equivalent[e]
AroA (wild type)	0.24 ± 0.001 (2)	24 ± 2		
AroAH6	0.25 ± 0.02 (8)	20 ± 2		
K22A	0.10 ± 0.03 (2)	0.17 ± 0.01	100	K22
K22R	0.11 ± 0.02 (2)	0.72 ± 0.20		
D49A	0.25 ± 0.01 (2)	9.8 (± 0.1) × 10^{-4}	100	D49
N94A	0.41 ± 0.01 (2)	11 ± 1	87	none
R100M	0.27 ± 0.01 (3)	0.044 ± 0.003	100	R91[f]
R124A	0.26 ± 0.01 (2)	4.7 (± 0.5) × 10^{-3}	99	R120
Q171A	0.10 ± 0.02 (2)	0.40 ± 0.11	99	none
Y200F	0.13 ± 0.01 (2)	0.24 ± 0.08	58	none
D313A	0.27 ± 0.02 (2)	0.10 ± 0.02	96	D305
D313N	0.20 ± 0.03 (2)	1.2 (± 0.7) × 10^{-3}		
K340A	0.27 ± 0.01 (3)	0.57 ± 0.18	90	none
E341A	0.34 ± 0.03 (9)	0.073 ± 0.010	99	C115
E341Q	0.25 ± 0.01 (2)	2.3 (± 0.4) × 10^{-3}		
R344K	0.07 ± 0.002 (2)	7.6 (± 1.2) × 10^{-3}	97	R331
R344M	0.22 ± 0.007 (2)	3.9 (± 0.9) × 10^{-3}		
H385A	0.30 ± 0.01 (2)	0.020 ± 0.001	96	L370
R386M	0.23 ± 0.01 (2)	3.8 (± 0.9) × 10^{-3}	100	R371
K411A	0.29 ± 0.01 (2)	2.5 ± 0.3	63	R397

[a] All side chain mutants contain the same C-terminal His_6-tag as $AroA_{H6}$. [b] *f*(PEP) = [[1-^{14}C]PEP]/([[1-^{14}C]PEP] + [[1-^{14}C]EPSP]). Values are reported with standard errors, except $AroA_{H6}$ and E341A, where there were enough independent determinations to calculate the 95% confidence interval. Numbers in parentheses are the number of independent measurements. [c] Reaction conditions: 3 mM S3P, 8 mM PEP, 50 mM Tris·HCl, pH 7.5, 100 mM KCl, 25 °C. Errors are the standard error in the fits to product-vs-time plots. Specific activities were calculated based on total protein concentration. [d] Percentage of 89 aligned AroA/EPSP synthase sequences containing the indicated amino acid at that position. The average conservation of the most common amino acid at any given position was 49% (alignment not shown). [e] On the basis of the sequence alignment and spatial superposition of *E. coli* AroA structures (PDB 1G6S, 1G6T) and *E. coli* MurA (1A2N, 1UAE). [f] Spatially equivalent residues that are not aligned with each other in the amino acid sequence and are contributed by different parts of the polypeptide chain: AroA_R100, MurA_R91; AroA_E341, MurA_C115; AroA_R344, and MurA_R331. Position of the MurA_R91 side chain had poor overlap with AroA_R100 and was variable between different MurA structures (1UAE and 1A2N). All remaining pairs of residues were both spatially superimposed and aligned with each other in the amino acid sequence.

[2] THI concentration was approximately 2 μM, based on the specific activity of ^{14}C in the THI. If $K_M \ll$ [THI], then the true k_{cat}/K_M would be higher than the calculated value.

measurable activity, as observed previously with petunia EPSP synthase (*35*). (ii) Unexpectedly, the C-terminal extension of $AroA_{H6}$ appeared to stabilize the protein. Previously, wild-type AroA was denatured and precipitated with 0.2 N NaOH and $CHCl_3$ (*4*). However, $AroA_{H6}$ required 0.4 N KOH/(33% KOH-saturated 2-propanol) and $CHCl_3$. It was active at pH 13 and retained activity after brief exposure to pH 14. Because of this stabilization, mutants may have retained activity where they would otherwise have been unable to fold. If this is true, the specific activities of mutants reported here would reflect changes in enzyme·substrate interactions to a greater extent than protein stability. (iii) The ^{33}P-assay made it possible to routinely use much higher substrate concentrations (8 mM S3P, 3 mM PEP) than in previous mutagenesis studies (*34*−*38*). Given the strong positive cooperativity of substrate binding (*33*), it was hoped that this would allow detection of even very weak activity. Also, relatively high ionic strength, $I = 0.15$, was maintained because substrate binding is ionic strength-dependent (ref *42* and unpublished data).

Specific activities were determined with 8 mM S3P, 3 mM PEP, 50 mM Tris·HCl, pH 7.5, 100 mM KCl, at 25 °C. Changes in specific activity may reflect changes in k_{cat} or k_{cat}/K_M or some combination of both. They reflect changes in TS stabilization, even if the exact meaning in terms of steady-state kinetic parameters is ambiguous.

THI Breakdown and Partitioning. On the basis of the concentration of mutant enzymes required to catalyze breakdown of most of the THI within 2 min, the rates of THI breakdown for all mutants were within a factor of 100 of $AroA_{H6}$. (The rate was measured only for $AroA_{H6}$.) This was despite decreases in specific activity of up to 21 000-fold for the overall reaction. This difference in behaviors between the THI and the overall reactions is not surprising: (i) THI breakdown is probably at least partially diffusion rate-limited, based on the very large k_{cat}/K_M, 1.4×10^8 M^{-1} s^{-1}. If the reaction is diffusion rate-limited, the chemical steps are not kinetically significant, and decreases in the rates of the chemical steps will be attenuated or even unobservable. (ii) The THI is very much less stable than the substrates or products; thus, the mechanistic imperatives for its breakdown are smaller, and even catalytically impaired mutants can degrade THI with good efficiency. (iii) There are two routes to THI breakdown. If the forward rate decreased, there would be an increased flux through the reverse reaction and vice versa. (iv) The AroA structure consists of two domains with a flexible hinge, with S3P interacting predominantly with the N-terminal domain[3] (*43*) and PEP interacting predominantly with the C-terminal domain. In contrast, THI contains all the atoms of S3P and PEP and can interact with both domains. This may help to form the active site with correctly positioned amino acids when interdomain contacts have been affected by mutations.

Partitioning factors, *f*(PEP) for AroA, $AroA_{H6}$, and all mutants were determined (Table 1, Figure 4). Partitioning was pH-independent at pH > 8, with $f(PEP) = 0.33 \pm 0.02$ (Figure 5). At low pH, *f*(PEP) decreased so that there was no detectable PEP formation below pH 6.0. The pH-dependence of *f*(PEP) fitted well to a single ionization with $pK_a = 6.97 \pm 0.06$.

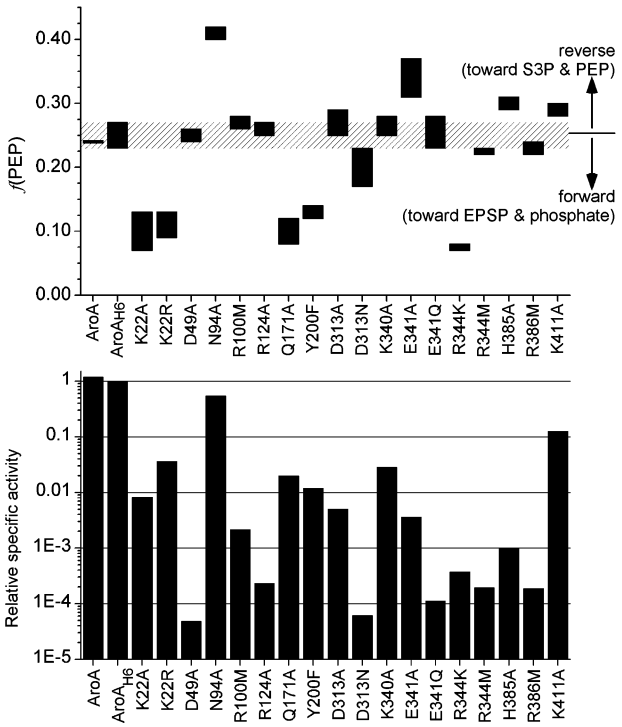

FIGURE 4: Characterization of AroA mutants. (a) Partitioning factors for wild type and mutant AroAs, *f*(PEP) = [[1-^{14}C]PEP]/([[1-^{14}C]-PEP] + [[1-^{14}C]EPSP]). Bars show the range of *f*(PEP) (i.e., average ± standard error or 95% confidence interval as applicable) (see Table 1). The hatched bar shows *f*(PEP) for $AroA_{H6}$. (b) Specific activities of mutants relative to $AroA_{H6}$.

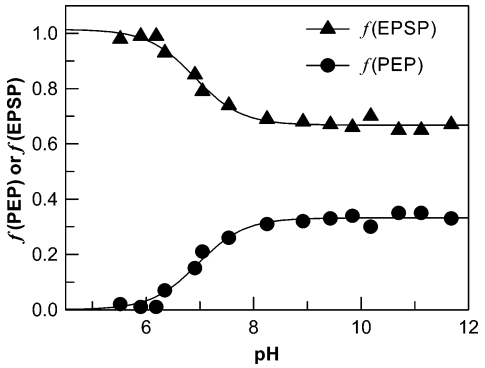

FIGURE 5: pH-dependence of partitioning. (●)—*f*(PEP) and (▲)—*f*(EPSP). The pH-dependence of both data sets fit to a single ionization with $pK_a = 6.97 \pm 0.06$. Values of *f*(PEP) and *f*(EPSP) were derived from the same experimental data.

Numerical Simulation of Partitioning Experiments. Because no step in the kinetic mechanism was cleanly rate-limiting or irreversible and all enzyme-bound species are partially equilibrated with each other (Figure 2), it was necessary to perform numerical simulations to interpret partitioning experiments. Systematically varying microscopic rate constants showed that the system behaves intuitively. That is, there was a change in partitioning only when there was a differential change in the TS energies in one branch of the reaction (i.e., forward or backward from the THI). If TS energies were increased equally in both branches, the rate decreased, but partitioning remained unchanged. Changing the energies of enzyme-bound species did not affect partitioning unless there was a corresponding change in TS

[3] N-terminal domain: residues 22−239. C-terminal domain: residues 1−21 and 240−427.

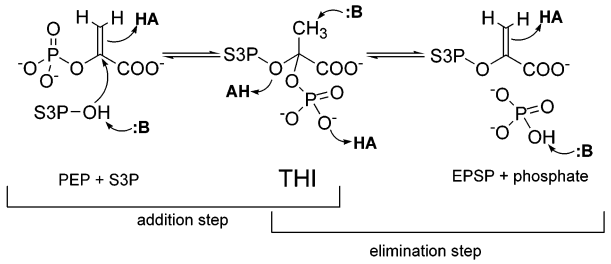

FIGURE 6: Mechanism of THI breakdown, showing potential general acid and general base catalysis. The reaction is freely reversible. The protonation states of phosphate and carboxylate are not known.

energies. Because of partial equilibration between all enzyme-bound species, an incremental change in a microscopic rate constant gave a smaller change in partitioning. For example, a 10-fold decrease in TS stabilization in the elimination step resulted in a 2.5-fold shift in *f*(PEP) from 0.17 to 0.42. Similarly, a 10-fold decrease in TS stabilization in the addition step resulted in a 2.3-fold shift in *f*(PEP) from 0.17 to 0.08.

DISCUSSION

Mechanistic Imperative of Carboxyvinyl Transfer. AroA and MurA catalyze carboxyvinyl transfer through an addition/elimination pathway, passing through a tetrahedral intermediate. A number of proton transfers are required that are subject to general acid and general base catalysis (Figure 6). Addition requires protonation of C3 of PEP and deprotonation of S3P O5′H. Elimination requires deprotonation of C3 and protonation of phosphate. THI breakdown in either direction is an elimination reaction, where either S3P O5′H or phosphate is protonated, and C3 is deprotonated.

Enzymatic general acid/base catalysis often supplies >6 kcal/mol of TS stabilization (*44*) (i.e., $>10^4$-fold rate enhancement) with rate enhancements as high as 10^8-fold reported (*45*). However, the effectiveness of acid/base catalysis in a particular step will depend on the exact mechanism. For example, in an A_NA_H mechanism[4] (*46*, *47*) where addition is concerted, with simultaneous protonation at C3 and nucleophilic attack at C2, both general acid and general base catalysis will be effective. However, for a stepwise $A_H + A_N$ mechanism forming a discrete cationic intermediate, general base catalysis may not be required because the cationic intermediate will be so electrophilic that it would react with S3P O5′H without prior deprotonation. Conversely, for a stepwise $A_N + A_H$ mechanism, initial nucleophilic attack forms a discrete anionic intermediate, and C3 would become so basic that little acid catalysis would be required. The same considerations apply for the elimination step, which could have a D_ND_H (E2), $D_N + D_H$ (E1), or $D_H + D_N$ (E1cB) mechanism. Reverse THI breakdown is also an elimination. Given the uncertainties regarding the mechanisms in each direction, it is difficult to know beforehand whether general acid or general base catalysis of a particular step will be effective.

Mutant AroAs. In an effort to identify residues involved in TS stabilization, all 14 amino acid side chains within 5 Å of a reactive atom from the THI in the AroA·THI model were mutated. (A reactive atom was defined as an atom originating from PEP, plus S3P O5′.) In all, 18 mutations were made.

Most of the mutations caused significant decreases in specific activity, with eight out of 18 having a >1000-fold decrease, but none caused extremely large decreases. Thus, the catalytic power of AroA resides in a large number of residues, an example of "ensemble catalysis". The concept of ensemble catalysis is especially appropriate when considering the roles of the general acid/general base catalysts. The catalytic enhancements attributed to Lys22 and Glu341 are modest as compared with values of up to 10^8 attributed to other acid/base catalysts (*45*), emphasizing the cumulative contributions of the other amino acids in the active site (see below).

Partitioning Analysis. The goal of partitioning analysis was to distinguish the contributions of individual amino acids to TS stabilization of either the addition or the elimination step. Previous mutagenesis studies identified certain amino acids in AroA (*34*, *35*, *37*, *38*, *40*) and MurA (*14*, *48*, *49*) as important, but activity assays could not differentiate between effects on addition versus elimination.

Possible values of *f*(PEP) range from 0 (THI goes completely forward to EPSP and phosphate) to 1 (back to S3P and PEP). The most striking result of the partitioning experiments was the lack of very large effects, with all values between *f*(PEP) = 0.07 and 0.41, as compared with 0.25 for $AroA_{H6}$. From numerical simulations, this range represents differential changes in microscopic rate constants of ≈15- and ≈4-fold, respectively. Mutations to residues acting as general acid or base catalysts would have been expected to significantly slow one step or the other, causing large changes in *f*(PEP).

The question arises, then, whether large changes in microscopic rate constants could be detected if they occurred. There are three pieces of evidence that they would be. (i) With $AroA_{H6}$, at pH < 6, there was no detectable [1-^{14}C]-PEP formation (i.e., *f*(PEP) = 0).[5] This shift occurred in a pH range where it has been shown previously that there is only modest catalytic impairment (*40*, *41*, *50*). (ii) The largest shift in partitioning in the backward direction occurred with mutant N94A, *f*(PEP) = 0.41, which had the smallest decrease in specific activity of any mutant, 1.8-fold. (iii) The largest shift in partitioning in the forward direction was R344K, *f*(PEP) = 0.07. Its specific activity was within a factor of 2 of R344M, which had a partitioning factor close to wild type, *f*(PEP) = 0.22. Presumably, the Lys side chain of R344K forms an interaction not present with Arg or Met. Thus, in three instances, relatively large changes in partitioning accompanied modest changes in specific activity, giving good confidence that if a mutation had caused large changes

[4] In IUPAC nomenclature, each elementary step of the reaction is indicated. Thus, A_NA_H corresponds to a concerted addition of a nucleophile and a proton, respectively. A plus (+) sign indicates a stepwise reaction where a discrete intermediate is formed between the elementary steps (e.g., $A_N + A_H$ and $A_H + A_N$). For elimination reactions, the corresponding elementary steps are bond dissociations, thus: D_ND_H, $D_N + D_H$, or $D_H + D_N$.

[5] The source of this shift in *f*(PEP) is unknown. As the fitted pK_a was similar to that expected for a phosphate monoester, it would be reasonable, a priori, to assume that phosphate protonation made it a better leaving group. However, recent results on nonenzymatic THI breakdown showed no rate dependence on the protonation state of nonbridging phosphate oxygens (unpublished data).

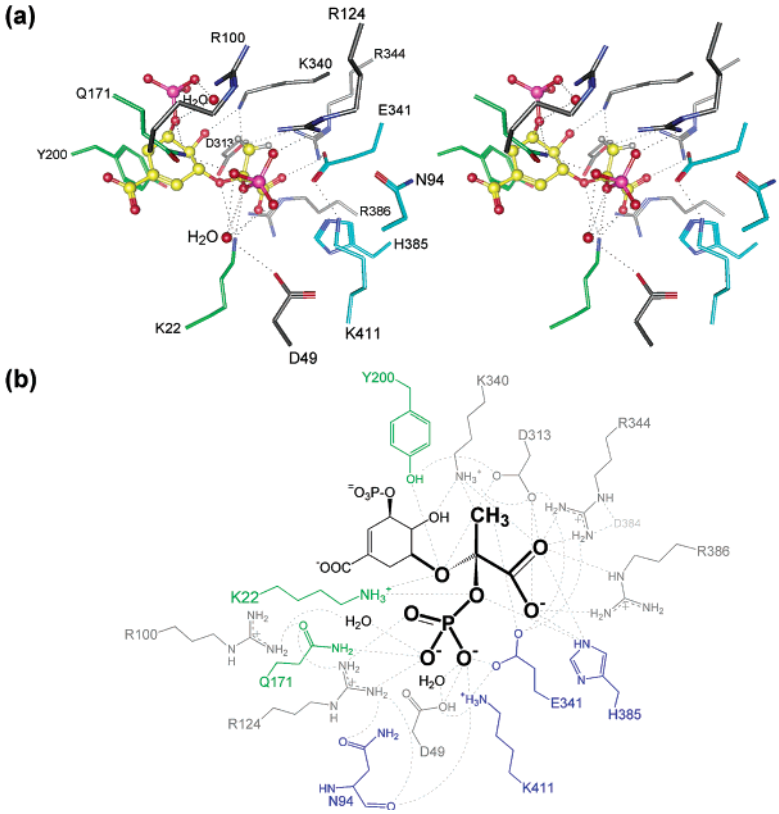

FIGURE 7: (a) Active site residues of the AroA·THI model complex. THI carbon atoms are yellow, and side chain carbons are colored according to effect of mutation on *f*(PEP): gray—no effect, green—*f*(PEP) ≤ 0.20, and cyan—*f*(PEP) ≥ 0.29. Potential hydrogen bonds are shown with dotted lines. The model was based on AroA and MurA cocrystal structures with inhibitor and/or substrate ligands (see text). (b) Schematic diagram of AroA·THI contacts. Amino acid colors are as for panel a. Dashed lines indicate contacts within 5 Å, the basis for selecting residues to mutate.

in TS stabilization in only the forward or reverse reaction, large changes in *f*(PEP) would have been observed.

Structure and Partitioning. There was a trend for *f*(PEP) to correlate with location within the active site (Figure 7). Two of three mutants with decreased *f*(PEP) make contact with the S3P portion of the THI, while the mutants with increased *f*(PEP) make contact with, or are close to, the PEP portion. This spatial distribution is especially striking because it involves residues from both the N-terminal (N94A) and the C-terminal (E341A, H385A, K411A) domains and side chains not in direct contact with the THI (N94A, H385A). This suggests that the shifts in *f*(PEP) arise from changes in protein structure and/or that the THI moves within the active site during catalysis. If, for example, EPSP interacts more strongly than the THI with residues 94, 341, 385, and 386 and if this stronger interaction is at least partly developed in the transition state, the effect of mutations would be to destabilize the transition state for elimination and cause *f*(PEP) to increase. Conversely, if S3P interacts more strongly with residues 171 and 200 in reverse THI breakdown, mutations could cause a decrease in *f*(PEP). K22A and K22R had low *f*(PEP)s, but it is not clear whether this is due to location or other factors (see below).

General Acid Catalysis of THI Breakdown. Effects of Mutations on f(PEP). THI breakdown would be expected to be general acid catalyzed to promote leaving group departure. The lack of large changes in *f*(PEP) could indicate (i) general acid catalysis is not required for leaving group departure (S3P O5′H or phosphate), (ii) the general acid catalyst was not among the mutated residues, or (iii) the same residue acts as general acid in both the forward and reverse breakdown of THI.

(i) Is Acid Catalysis Necessary? In general, leaving group departure is acid catalyzed, and there are many examples of acid catalysis of leaving group departure through protonation of ether and acetal (*51*) oxygens. Phosphate departure through C−O bond cleavage in nonenzymatic breakdown of AroA and MurA THIs is general acid catalyzed (unpublished data and ref *6*), as well as in other phosphates (*52*). There is little direct evidence for general acid catalysis in AroA; however, the observed acid catalysis in nonenzymatic THI breakdown shows that it is probable.

(ii) General Acid Catalyst Among Mutated Residues? Every amino acid within 5 Å of a reactive atom in the AroA·THI model was mutated, including side chains not in direct contact with the THI. It is highly unlikely that a general acid catalyst could exist but not be one of the mutated side chains.

(iii) One General Acid Catalyst for Both Leaving Groups? If one amino acid residue were acting as general acid in both the forward and the reverse reactions, then the effects of mutation on *f*(PEP) would be modest, as the reaction in both directions would be affected roughly equally. One candidate for this role is Lys22.

Invariance of f(PEP) at High pH. More evidence for a single general acid catalyst came from the fact that *f*(PEP) was constant between pH 8 and 11.7 (Figure 5). The invariance with pH is consistent with a single acid catalyst. If only one catalyst is present, then the rate will slow as it becomes deprotonated at high pH, but *f*(PEP) will not change because both steps will be affected equally. Unchanging

f(PEP) at high pH is consistent with one amino acid acting as general acid catalyst for both S3P and phosphate departure in THI breakdown.

Lys22 as a General Acid Catalyst. Lys22 is a candidate general acid catalyst in THI breakdown. In the AroA·S3P·glyphosate, AroA·S3P·phosphate·formate, and AroA·THI structures, Lys22 N_ζ was in contact with S3P, at least one oxygen of the phosph(on)ate, and a carboxylate oxygen of glyphosate, formate, or THI (Figure 7). Lys22 was situated to donate a proton to either the O5′ or the phosphate in the THI.

In the overall reaction, it would be a general base during addition deprotonating S3P O5′H, and then a general acid during elimination protonating the departing phosphate with little or no side chain movement. In K22A and K22R *f*(PEP) = 0.1, which may be rationalized by noting that S3P O5′H is a worse leaving group because of its higher pK_a, meaning that S3P departure would be affected more than phosphate in the mutants. The 2.5-fold decrease in *f*(PEP) represents a ≈10-fold differential decrease in TS stabilization of S3P departure.

Three lines of evidence (small effect of mutation on *f*(PEP), invariance of *f*(PEP) at high pH, appropriate location) point toward Lys22 being the general acid catalyst in THI breakdown in both directions. The specific activity of K22A decreased 120-fold, a relatively modest change, but not unprecedentedly so. This represents an increase in free energy of activation, $\Delta\Delta G^{\ddagger}$, of 2.8 kcal/mol. Modest catalytic enhancements have been observed with other enzymatic general acid catalysts (*53*, *54*). The catalytic enhancement possible by Lys22 will depend on the exact mechanism. A mechanism involving formation of a discrete cationic intermediate may require little or no general acid catalysis, as discussed above. The large number of positively charged side chains in the active site could provide significant electrostatic stabilization of leaving group departure.

If Lys22 is a general acid catalyst in THI breakdown, this implies it will act as a general base catalyst to deprotonate S3P O5′H. The estimated pK_a of Lys22, 7.6 (*55*), is lower than a normal Lys side chain (pK_a ≈ 10.5), ensuring that there is a significant concentration of the neutral form at physiological pH to act as a general base.

Ensemble catalysis implies that the enzyme is still capable of significant TS stabilization even in the absence of the acid catalyst. K22R had higher specific activity than K22A, presumably because Arg can provide some electrostatic stabilization to compensate for the loss of Lys.

General Base Catalysis of THI Breakdown. THI breakdown requires deprotonation of C3, making it subject to general base catalysis. We have identified Glu341 as a candidate general base catalyst, as proposed previously based on the AroA X-ray crystal structure (*18*). In the addition step of the overall reaction, it would act as the general acid to protonate C3.

The stereochemistries of the AroA (*56*−*58*) and MurA (*11*, *12*, *59*) reactions have been characterized extensively. Glu341 is correctly located to catalyze the required anti addition (with proton transfer to the 2-*si* face of PEP) followed by syn elimination. The opposite stereochemistries of addition and elimination (anti/syn) makes it possible for a single amino acid to protonate PEP and deprotonate the THI.

Glu341 is nearly superposed with MurA_C115 in AroA and MurA structures despite the fact that these residues occur in different domains of the proteins. Cys115 S_γ was within 0.8 Å of Glu341 C_δ in the superposed structures of AroA·S3P·glyphosate (*18*) and MurA-fosfomycin·UDP-GlcNAc (*17*). *E. coli* MurA_C115 is the proposed general acid/base catalyst that protonates and deprotonates PEP C3 (*8*, *11*). Asp replaces Cys115 in nine of the 48 known MurA sequences, demonstrating that a carboxylate is functional in this position. In the AroA·THI model, Glu341 could interact with the THI through a nonbridging phosphate oxygen ($d_{O\cdots O}$ = 2.8 Å) and/or C3 ($d_{O\cdots C}$ = 4.2 Å). The distance to C3 is large and the phosphate···carboxyl(ate) contact is poorly oriented, but this is not a serious problem given the accuracy of the AroA·THI model and the likelihood of motions during catalysis.

Two mutations were made to this residue, E341A and E341Q. There was a modest increase in *f*(PEP) to 0.34 with E341A, while E341Q was the same as $AroA_{H6}$. The specific activities decreased 280- and 9000-fold, respectively, with $\Delta\Delta G^{\ddagger}$ = 3.3 and 5.3 kcal/mol. The decrease in specific activity from E341A to E341Q could have arisen from two sources. (i) If water partly replaced the function of Glu in E341A, it would be displaced in E341Q, which is isosteric with Glu, preventing water from binding while being unable to act as a general base itself. (ii) It is also possible that the carboxamide $-NH_2$ of Gln could introduce unfavorable interactions not present in $AroA_{H6}$ or E341A.

The possibility has been advanced that the THI phosphate could catalyze its own elimination by acting as a general base to deprotonate C3 of the THI (*11*). Such a syn elimination is reasonable a priori; one of the phosphate oxygens can be positioned in van der Waals' contact of a C3 proton. However, it could not catalyze S3P departure because proton abstraction would be orthogonal to the scissile C−O bond, slowing the reaction by as much as 10^{10}-fold because of stereoelectronic effects (*60*, *61*). If phosphate catalyzed its own departure, another amino acid would have to act as a general base for S3P departure, which would have been evident from an experimental *f*(PEP) becoming 0 because removing this base catalyst would cause partitioning to shift completely in the forward direction.

There are no other good candidates for the role of general acid/base catalyst. In AroA·THI, Asp313 had a carboxylate oxygen located within 3.5 Å of C3, and the behavior of the D313A and D313N mutants was very similar to the Glu341 mutants. However, if it were a general acid/base catalyst, the absolute stereochemistry of protonation/deprotonation would be incorrect, with proton addition to the 2-*re* face of PEP rather than 2-*si*.

Dual Role Acid/Base Catalysts. Both Lys22 and Glu341 are proposed to act as both acid and base catalysts in different steps of the reaction. It is common for single residues to act as both acid and base in a single catalytic cycle (*44*, *62*, *63*). In this regard, the proposed dual roles of Lys22 and Glu341 is consistent with the mechanisms of many, or most, enzymes.

Mutations to Phosphate-Binding Residues. Several of the mutated amino acids were close to the THI phosphate: Asp49, Arg100, Arg124, and Lys411. Except for K411A (3-fold), these mutations caused large decreases in specific activity, but none caused large changes in *f*(PEP) in either

direction. This was the expected effect based on our recent results showing that the protonation state of the nonbridging phosphate oxygens of the THI do not affect rate of nonenzymatic THI breakdown (unpublished data).

Arg100 does not make direct contact with the THI in the model structure, implying a role in protein stability or conformation, consistent with the 400-fold reduction in the yield of purified protein. D49A was the most deleterious mutation, with a 21 000-fold decrease in specific activity. Asp49 is invariant in both AroA and MurA sequences. It does not make direct contact with the phosphate but may interact with the nonbridging oxygens through a water molecule. This water is present in the AroA·S3P·glyphosate and AroA·S3P·phosphate structures, as well as MurA-fosfomycin·UDP-GlcNAc and MurA·F-THI. The exact role of Asp49 is not clear. It may act through its water-mediated interaction with the phosphate or indirectly by controlling protein stability or conformation. The yield of purified D49A was 0.5% of $AroA_{H6}$, suggesting that it may be important for protein stability.

Other Mutants. Gln171 and Tyr200 appear to interact primarily with the S3P portion of the THI, as reflected in the change in *f*(PEP) upon mutation. In both cases, the effect on specific activity was relatively small, 50- and 80-fold, respectively.

Mutants close to the O1 carboxylate oxygens, R344K/M, H385A, and R386M, had reduced specific activities by 1000−5000-fold. Previous studies reported that H385A retained 1% of wild-type activity, while H385N and H385Q had 6 and 25% of wild-type activity, respectively (*40*, *41*). The reason for the discrepancy in specific activities is not clear, but the higher activity of H385Q shows that the acid/base properties of His385 are not essential for catalysis. The guanidino group of Arg386 was not well-oriented to interact with the THI C1 carboxylate in the AroA·THI model; however, this likely represents a shortcoming of the model as it is ideally oriented in the crystal structures.

AroA_D313 was advanced previously as a general base catalyst for THI formation (*18*), as was the analogous residue MurA_D305 (*48*). Its location would preclude protonating phosphate in the elimination step, so the lack of large effect on *f*(PEP) in D313A or D313N argues against it being the general base catalyst. The effects of mutations at Asp313 were similar to Glu341, with specific activity decreasing by factors of 200 (D313A) and 16 000 (D313N). The decreased activity of D313N relative to D313A could arise from the same causes as E341Q relative to E341A, namely, displacement of water substituting for Asp, or new, inhibitory interactions through the $-NH_2$ of Asn. AroA_D313 fulfills an important, as yet unknown, role in catalysis, but the lack of effect on *f*(PEP) argues against it being the general base in the addition step.

Comparison with MurA. The amino acid sequences of *E. coli* AroA and MurA are highly divergent, with only 19% identity (alignment not shown). Most of the amino acids mutated in this study are conserved in MurA or have structural analogues—residues with the same or similar functional groups that appear in the same position in space but not in the sequence (Table 1). One of these superimposed but unaligned residues was MurA_C115, which occupied the same position in space as AroA_E341, the proposed general base in THI breakdown.

Lys22 is 100% conserved in both AroA and MurA sequences. In the MurA structures, the relative disposition of Lys22 and ligands was different. Whereas AroA_K22 N_ζ was within hydrogen bonding distance of both S3P O5′ (2.8−3.0 Å) and the phosphate oxygen O2 (2.9 Å), the distance to O3″ of UDP-GlcNAc in MurA was 4.4−5.2 Å. MurA_D305, the analogue of AroA_D313, has been proposed to be the base catalyst that deprotonates O3″ in the addition step (*48*), the role that we propose is fulfilled by AroA_K22. Given the differences in the position of Lys22 in AroA and MurA, it is conceivable that it, along with Asp313(305), plays different roles in the catalytic mechanisms of AroA and MurA despite their similar locations in the active site.

CONCLUSIONS

The catalytic mechanism of *E. coli* AroA was examined through partitioning analysis and the specific activity of a large number of site specific mutants. Partitioning analysis (i.e., determining the fate of purified THI added back to $AroA_{H6}$ and its mutants) provided evidence for one amino acid residue, Lys22, acting as the general acid catalyst of THI breakdown in both the forward and the reverse reactions, while Glu341 acts as the general base. Thus, in the addition step of the overall forward reaction, Lys22 would act as a general base catalyst to deprotonate S3P O5′H while Glu341 would act as general acid to protonate C3 of PEP.

Of the 18 mutations examined, eight resulted in >1000-fold decreases in specific activity, demonstrating that a large number of amino acid residues contribute to catalysis. This suggests that AroA acts by ensemble catalysis, with a large number of amino acids contributing to catalysis but no single amino acid being absolutely required. The relatively modest catalytic enhancements attributable to the proposed general acid and general base catalysts emphasizes the contribution of a large number of amino acids in TS stabilization. Ensemble catalysis makes it more difficult to predict the exact mechanisms of the addition and elimination steps or the structures of the transition states. TS analysis using multiple kinetic isotope effects will provide detailed experimental TS structures, yielding new insights into the mechanism of AroA.

ACKNOWLEDGMENT

We thank Prof. Debra Dunaway-Mariano (University of New Mexico) for a generous gift of pyruvate phosphate dikinase, Prof. Luiz Basso (Universidade Federal do Rio Grande do Sul, Brazil) for the gift of *E. coli* overexpressing AroK, Ming-Hua Wang for technical assistance in early parts of this study, and Anna Oddone for assistance in producing $AroA_{H6}$.

SUPPORTING INFORMATION AVAILABLE

Mutagenesis strategy, amino acid and DNA sequences of $AroA_{H6}$ and mutants, and experimental M_rs. This material is available free of charge via the Internet at http://pubs.acs.org.

REFERENCES

1. Sikorski, J. A., and Gruys, K. J. (1997) *Acc. Chem. Res. 30*, 2−8.
2. Hendlin, D., Stapley, E. O., Jackson, M., Wallick, H., Miller, A. K., Wolf, F. J., Miller, T. W., Chaiet, L., Kahan, F. M., Foltz, E.

L., Woodruff, H. B., Mata, J. M., Hernandez, S., and Mochales, S. (1969) *Science 166*, 122−123.
3. Anderson, K. S., and Johnson, K. A. (1990) *Chem. Rev. 90*, 1131−1149.
4. Anderson, K. S., Sammons, R. D., Leo, G. C., Sikorski, J. A., Benesi, A. J., and Johnson, K. A. (1990) *Biochemistry 29*, 1460−1465.
5. Anderson, K. S., Sikorski, J. A., and Johnson, K. A. (1988) *Biochemistry 27*, 7395−7406.
6. Anderson, K. S., and Johnson, K. A. (1990) *J. Biol. Chem. 265*, 5567−5572.
7. Anderson, K. S., Sikorski, J. A., Benesi, A. J., and Johnson, K. A. (1988) *J. Am. Chem. Soc. 110*, 6577−6579.
8. Kim, D. H., Lees, W. J., Kempsell, K. E., Lane, W. S., Duncan, K., and Walsh, C. T. (1996) *Biochemistry 35*, 4923−4928.
9. Kim, D. H., Lees, W. J., and Walsh, C. T. (1994) *J. Am. Chem. Soc. 116*, 6478−6479.
10. Marquardt, J. L., Brown, E. D., Lane, W. S., Haley, T. M., Ichikawa, Y., Wong, C. H., and Walsh, C. T. (1994) *Biochemistry 33*, 10646−10651.
11. Skarzynski, T., Kim, D. H., Lees, W. J., Walsh, C. T., and Duncan, K. (1998) *Biochemistry 37*, 2572−2577.
12. Lees, W. J., and Walsh, C. T. (1995) *J. Am. Chem. Soc. 117*, 7329−7337.
13. Eschenburg, S., and Schonbrunn, E. (2000) *Proteins 40*, 290−298.
14. Schonbrunn, E., Eschenburg, S., Krekel, F., Luger, K., and Amrhein, N. (2000) *Biochemistry 39*, 2164−2173.
15. Schonbrunn, E., Eschenburg, S., Luger, K., Kabsch, W., and Amrhein, N. (2000) *Proc. Natl. Acad. Sci. U.S.A. 97*, 6345−6349.
16. Schonbrunn, E., Sack, S., Eschenburg, S., Perrakis, A., Krekel, F., Amrhein, N., and Mandelkow, E. (1996) *Structure 4*, 1065−1075.
17. Skarzynski, T., Mistry, A., Wanacott, A., Hutchinson, S. E., Kelly, V. A., and Duncan, K. (1996) *Structure 4*, 1465−1474.
18. Schonbrunn, E., Eschenburg, S., Shuttleworth, W. E., Schloss, J. V., Amrhein, N., Evans, J. N. S., and Kabsch, W. (2001) *Proc. Natl. Acad. Sci. U.S.A. 98*, 1376−1380.
19. Stallings, W. C., Abdel-Meguid, S. S., Lim, L. W., Shieh, H.-S., Dayringer, H. E., Leimgruber, N. K., Stegeman, R. A., Anderson, K. S., Sikorski, J. A., Padgette, S. R., and Kishore, G. H. (1991) *Proc. Natl. Acad. Sci. U.S.A. 88*, 5046−5050.
20. Albery, W. J., and Knowles, J. R. (1976) *Biochemistry 15*, 5627−5631.
21. Mehl, A., Xu, Y., and Dunaway-Mariano, D. (1994) *Biochemistry 33*, 1093−1102.
22. Shuttleworth, W. A., Hough, C. D., Bertrand, K. P., and Evans, J. N. S. (1992) *Protein Eng. 5*, 461−466.
23. Edelhoch, H. (1967) *Biochemistry 6*, 1948−1954.
24. Pace, C. N., Vajdos, F., Fee, L., Grimsley, G., and Gray, T. (1995) *Protein Sci. 4*, 2411−2423.
25. Anderson, K. S., Sikorski, J. A., and Johnson, K. A. (1988) *Biochemistry 27*, 1604−1610.
26. Castellino, S., Leo, G. C., Sammons, R. D., and Sikorski, J. A. (1991) *J. Org. Chem. 56*, 5176−5181.
27. Roossien, F. F., Brink, J., and Robillard, G. T. (1983) *Biochim. Biophys. Acta 760*, 185−187.
28. Parra, F. (1982) *Biochem. J. 205*, 643−645.
29. Lanzetta, P. A., Alvarez, L. J., Reinach, P. S., and Candia, O. A. (1979) *Anal. Biochem. 100*, 95−97.
30. Halgren, T. A. (1996) *J. Comput. Chem. 17*, 490−519.
31. Barshop, B. A., Wrenn, R. F., and Frieden, C. (1983) *Anal. Biochem. 130*, 134−145.
32. Gruys, K. J., Marzabadi, M. R., Pansegrau, P. D., and Sikorski, J. A. (1993) *Arch. Biochem. Biophys. 304*, 345−351.
33. Gruys, K. J., Walker, M. C., and Sikorski, J. A. (1992) *Biochemistry 31*, 5534−5544.
34. Shuttleworth, W. A., Pohl, M. E., Helms, G. L., Jakeman, G. L., and Evans, J. N. S. (1999) *Biochemistry 38*, 296−302.
35. Huynh, Q. K., Bauer, S. C., Bild, G. S., Kishore, G. M., and Borgmeyer, J. R. (1988) *J. Biol. Chem. 263*, 11636−11639.
36. Selvapandiyan, A., Majumder, K., Fattah, F. A., Ahmad, S., Arora, N., and Bhatnagar, R. K. (1995) *FEBS Lett. 374*, 253−256.
37. Padgette, S. R., Re, D. B., Gasser, C. S., Eichholtz, D. A., Frazier, R. B., Hironaka, C. M., Levine, E. B., Shah, D. M., Fraley, R. T., and Kishore, G. M. (1991) *J. Biol. Chem. 266*, 22364−22369.
38. Selvapandiyan, A., Ahmad, S., Majumder, K., Arora, N., and Bhatnagar, R. K. (1996) *Biochem. Mol. Biol. Int. 40*, 603−610.
39. Majumder, K., Selvapandiyan, A., Fattah, F. A., Arora, N., Ahmad, S., and Bhatnagar, R. K. (1995) *Eur. J. Biochem. 229*, 99−106.
40. Shuttleworth, W. A., and Evans, J. N. S. (1994) *Biochemistry 33*, 7062−7068.
41. Shuttleworth, W. A., and Evans, J. N. S. (1996) *Arch. Biochem. Biophys. 334*, 37−42.
42. Du, W., Liu, W. S., Payne, D. J., and Doyle, M. L. (2000) *Biochemistry 39*, 10140−10146.
43. Stauffer, M. E., Young, J. K., Helms, G. L., and Evans, J. N. (2001) *FEBS Lett. 499*, 182−186.
44. Richard, J. P. (1998) *Biochemistry 37*, 4305−4309.
45. Carlow, D. C., Short, S. A., and Wolfenden, R. (1996) *Biochemistry 35*, 948−954.
46. Guthrie, R. D., and Jencks, W. P. (1989) *Acc. Chem. Res. 22*, 343−349.
47. March, J. (1992) *Advanced Organic Chemistry*, 4th ed., Wiley-Interscience, New York.
48. Samland, A. K., Etezady-Esfarjani, T., Amrhein, N., and Macheroux, P. (2001) *Biochemistry 40*, 1550−1559.
49. Samland, A. K., Amrhein, N., and Macheroux, P. (1999) *Biochemistry 38*, 13162−13169.
50. Steinrucken, H. C., and Amrhein, N. (1984) *Eur. J. Biochem. 143*, 341−349.
51. Capon, B. (1969) *Chem. Rev. 69*, 407−498.
52. Wolfenden, R., Ridgway, C., and Young, G. (1998) *J. Am. Chem. Soc. 120*, 833−834.
53. Frandsen, T. P., Dupont, C., Lehmbeck, J., Stoffer, B., Sierks, M. R., Honzatko, R. B., and Svensson, B. (1994) *Biochemistry 33*, 13808−13816.
54. Denu, J. M., Zhou, G., Guo, Y., and Dixon, J. E. (1995) *Biochemistry 34*, 3396−3403.
55. Huynh, Q. K., Kishore, G. M., and Bild, G. S. (1988) *J. Biol. Chem. 263*, 735−739.
56. Grimshaw, C. E., Sogo, S. G., Copley, S. D., and Knowles, J. R. (1984) *J. Am. Chem. Soc. 106*, 2699−2700.
57. Lee, J. J., Asano, Y., Shieh, T.-L., Spreafico, F., Lee, K., and Floss, H. G. (1984) *J. Am. Chem. Soc. 106*, 3367−3368.
58. Kim, D. H., Tucker-Kellogg, G. W., Lees, W. J., and Walsh, C. T. (1996) *Biochemistry 35*, 5435−5440.
59. Kim, D. H., Lees, W. J., and Walsh, C. T. (1995) *J. Am. Chem. Soc. 117*, 6380−6381.
60. Briggs, A. J., Evans, C. M., Glenn, R., and Kirby, A. J. (1983) *J. Chem. Soc., Perkin Trans. 2*, 1637−1640.
61. Perrin, C. L. (2002) *Acc. Chem. Res. 35*, 28−34.
62. Fersht, A. R. (1985) *Enzyme structure and mechanism*, 2nd ed., W. H. Freeman and Co., New York.
63. Zechel, D. L., and Withers, S. G. (2000) *Acc. Chem. Res. 33*, 11−18.

BI027217L